Published in final edited form as:
ACS Chem Biol. 2013 February 15; 8(2): 336–344. doi:10.1021/cb300542k.

Human DNA polymerase β, but not λ, can bypass a 2-deoxyribonolactone lesion together with proliferating cell nuclear antigen

Emmanuele Crespan[1], **Emanuela Pasi**[1], **Shuhei Imoto**[2], **Ulrich Hübscher**[3], **Marc M. Greenberg**[2], and **Giovanni Maga**[1]

[1]Institute of Molecular Genetics IGM-CNR, via Abbiategrasso 207, I-27100 Pavia (Italy) [2]Department of Chemistry, Johns Hopkins University, 3400 N. Charles St., Baltimore, MD 21218 (USA) [3]Institute of Veterinary Biochemistry and Molecular Biology, University of Zürich-Irchel, Winterthurerstrasse 190, CH-8057 Zürich (Switzerland)

Abstract

The C1′-oxidized lesion 2-deoxyribonolactone (L) is induced by free radical attack of DNA. This lesion is mutagenic, inhibits base excision repair, and can lead to strand scission. In double stranded DNA L is repaired by long-patch base excision repair, but it induces replication fork arrest in a single-strand template. Translesion synthesis requires a specialized DNA polymerase (Pol). In *E. coli,* Pol V is responsible for bypassing L, while in yeast Pol ζ has been shown to be required for efficient bypass. Very little is known about the identity of human Pols capable of bypassing L. For instance, the activity of family X enzymes has never been investigated. We examined the ability of different family X Pols: Pols β, λ and TdT from human cells and Pol IV from S. *cerevisiae* to act on DNA containing an isolated 2-deoxyribonolactone, as well as when the lesion comprises the 5′-component of a tandem lesion. We show that Pol β, but not Pol λ, can bypass a single L lesion in the template, and its activity is increased by the auxiliary protein proliferating cell nuclear antigen (PCNA), while both enzymes were completely blocked by a tandem lesion. Yeast Pol IV was able to bypass the single L and the tandem lesion but with little nucleotide insertion specificity. Finally, L did not affect the polymerization activity of the template-independent enzyme TdT.

Oxidized abasic residues (e.g. L, Figure 1A) are formed as a consequence of the exposure of DNA to oxidative agents. Among them, the C1′-oxidized abasic site 2-deoxyribonolactone (L) is a commonly observed lesion induced by ionizing- or long wave UV irradiation, organometallic oxidants and by antitumor drugs, such as neocarzinostatin and C1027 (1–4). In human cells, when present in double-stranded (ds) DNA, L is recognized by the base excision repair (BER) enzyme AP endonuclease 1, which generates an oxidized 5′-terminal residue. Further repair is impaired by the ability of this 5′-oxidized end to form protein-DNA crosslinks with the BER enzymes (5–8). Thus, L repair must be accomplished by the long patch BER sub-pathway, involving strand displacement followed by removal of the strand containing the 5′-oxidized residue by the flap endonuclease 1 (9–11). Persistence of L during S-phase, can cause replication fork arrest when the lesion is present on the template strand. Bypass of L has been shown to occur *in vivo* in *E. coli*, mainly due to the action of the translesion synthesis enzyme DNA polymerase (Pol V), leading to incorporation of dATP or dGTP opposite the lesion (2). Genetic data indicated that in yeast the specificity for L bypass was slightly different, with dCTP and dATP being the nucleotides most frequently inserted opposite L, and suggested that the Rev1 and Pol ζ enzymes were involved in translesion synthesis across the lesion (3).

To our knowledge, very little is known about the translesion capabilities of human Pols with respect to L. Previously, we showed that the two major BER enzymes in human cells, Pol β and Pol λ, efficiently bypass an AP site, but with different mechanisms (12). Pol λ more frequently skipped the lesion, using the downstream base as a template and generating −1 frameshift deletions. Pol β, on the other hand, preferentially incorporated dATP opposite an AP site. We have also shown that with the assistance of the auxiliary protein proliferating cell nuclear antigen (PCNA) DNA pol λ is very efficient in bypassing common oxidative lesions such as thymine glycol (Tg) (13), 2-hydroxyadenine (14), and 8-oxoguanine (15) in an error-free manner. Thus, we were interested in investigating the ability of Pol λ and Pol β to bypass a L lesion on the template, together with PCNA. Since fidelity and DNA synthesis efficiency of Pol β and λ are influenced by the nature of the metal activator, either Mg^{2+} or Mn^{2+} (16, 17), we studied the translesion synthesis across L in the presence of both metals. We have extended this analysis to the template-independent enzyme TdT, belonging to Pol family X (18) together with Pol λ and Pol β, and to the only member of the X family present in yeast, Pol IV (18). Finally, we compared translesion synthesis past a single L site, to the tandem lesion 5′-LTg (Figure 1B). Our data revealed distinct features for the different X family Pols in bypassing an L site.

Results and Discussion

We first analyzed the ability of Pol λ to bypass a L lesion *in vitro*. Initially, we compared the lesion bypass capacity of the enzyme as a function of the nucleotide concentration, on a 15/30mer heteropolymeric DNA substrate containing either a native nucleotide or a single L lesion at position +1 from the 3′-OH of the primer (Chart 1, **2**). In contrast to when an AP site was present in the template strand, Pol λ was unable to bypass L even in the presence of high concentrations (10 – 100 μM) of nucleotides and using either Mn^{2+} or Mg^{2+} as cofactors (data not shown). Like Pol β, Pol λ exhibits higher affinity for DNA containing a gap of a few nucleotides with a phosphorylated 5′ downstream end (19). However, we did not observe any nucleotide incorporation opposite the lesion (Figure 1C, lanes 1–5) when we tested the ability of Pol λ to bypass L when the lesion is opposite a single nucleotide gap (Chart 1, **4**). In contrast, robust gap filling and strand displacement synthesis took place as previously observed (20) (lane 7) with an otherwise identical template containing a native nucleotide in the same position (Chart 1, **3**).

In addition to the polymerase domain and the dRP-lyase domain, Pol λ possesses an N-terminal BRCT and proline-rich domain, responsible for protein-DNA and protein-protein interactions (18). Deleting this latter domain decreases fidelity (21). Consequently, the lesion bypass activity was investigated using a truncated form of Pol λ (Δ 1-243) in which only the catalytic domain, consisting of residues from 244 to 575, was maintained. However the Δ 1-243 was also unable to incorporate any nucleotide opposite the lesion either using Mn^{2+} or Mg^{2+} as cofactors and either substrate **2** or **4** (data not shown). PCNA, which promotes the translesion activity of Pol λ past an AP site (22), also did not confer the enzyme with the ability to synthesize DNA past the 2-deoxyribonolactone lesion. RP-A alone or in combination with PCNA was also unable to increase the activity of Pol λ when the template contained L (data not shown). Overall, these data clearly indicated that L showed more significant blocking properties compared to an AP site in the context of Pol λ translesion synthesis.

Pol β usually incorporates dCTP more frequently than dATP when it bypasses an AP site (12). When challenged with a L lesion (**2**), Pol β was able to bypass it but only using Mn^{2+} as cofactor. No translesion synthesis was observed with Mg^{2+} (data not shown). Contrary to the AP site, Pol β preferentially incorporated dATP opposite the L lesion, and with less efficiency dCTP (Figure 1D, lane 1–2 and 3–4 respectively). A barely detectable level of

dGTP incorporation was observed (lanes 5–6). Reaction performed with four nucleotides (Figure 1D, lane 9–10) resulted in full length products but with strong pausing at the site opposite to the lesion, with respect to the reaction performed using the undamaged substrate **1** (Figure 1D. Compare +1 products in lane 10 and 12), suggesting a poor elongation efficiency from the nucleotide paired with the L lesion on this template.

In order to determine the kinetic parameters of dATP incorporation, the nucleotide concentration was varied at fixed concentration of **1** or **2**, respectively (Figure 1E). The presence of the lesion caused a 4-fold reduction of the efficiency (Vm/Km) of the reaction when compared to the reaction performed using the undamaged substrate (Table 1).

To determine if primer extension performed by Pol β past a L lesion resulted in a −1 frameshift, we carried out incorporation reactions on **2**, containing different combinations of nucleotides (Figure 1F). Reaction performed with dATP only resulted in +1 product (lanes 1, 6). When dGTP was also added, +3 product appeared (lanes 2, 7), while addition of dGTP and dTTP resulted in +4 product (lanes 3, 8). The reaction performed employing all four nucleotides resulted in full-length product (lanes 5, 10). Single nucleotide deletion products were not observed in any of the reactions, excluding a −1 frameshift mechanism for L bypass by Pol β.

Pol β also shows higher nucleotide incorporation efficiency on DNA templates containing a gap of a few nucleotides with a phosphorylated 5′ downstream end. Indeed, when acting on **4** harboring a single nucleotide gap opposite the lesion (Figure 2A), Pol β exhibited more promiscuous translesion synthesis capabilities compared to the substrate **2** without gap. Specifically, in the presence of Mn^{2+}, besides dATP (Figure 2A, lane 6) and dCTP (Figure 2A, lane 7), Pol β incorporated dTTP (Figure 2A, lane 9), albeit with lower efficiency. Furthermore, when using Mg^{2+} as a cofactor along with this substrate (Figure 2A, lanes 1–4) the enzyme incorporated dATP and dCTP, but not dTTP. As apparent from the kinetic studies (Figures 2B, 2C and Table 1), with both metal ions Pol β incorporated dATP more efficiently than dCTP (~2.5-fold). When all four dNTPs were included in the reaction, limited strand displacement was observed in the presence of Mn^{2+} (Figure 2A, lane 10), which was further reduced in the presence of Mg^{2+} (Figure 2A, lane 5). On the contrary, on the undamaged **3** strand displacement was more robust and also occurred in the presence of Mg^{2+} (Figure 2A, lanes 11, 12). The presence of the lesion strongly affected the reaction efficiency, with a ~10-fold reduction when dATP incorporation was compared between undamaged and L damaged substrates using Mg^{2+} as cofactor, and ~20-fold reduction using Mn^{2+} (Table 1). These results suggest that the lesion L strongly reduces the efficiency of Pol β in filling a single nucleotide gap, also affecting its strand displacement activity.

PCNA physically interacts with Pol β (23) enhancing its bypass of AP sites (24). However, under single-nucleotide incorporation conditions, PCNA had no effect on dATP incorporation opposite L either on **2** (data not shown) or **4** (Figure 2D). The activity was independent of the identity of the metal cofactor. In contrast, in the presence of dATP (to be incorporated opposite the lesion) and dGTP (to allow further extension), PCNA enhanced the efficiency of Pol β elongation from the nucleotide opposite the lesion (Figure 2E) using the substrate **2** and Mn^{2+} as the metal cofactor. From the dependence of the reaction velocity on PCNA concentration, an apparent dissociation constant of 160 ± 20 nM for the PCNA-Pol β complex was derived, suggesting a stable interaction (Figure 2F).

Tandem lesions consist of two contiguously damaged nucleotides that are mainly generated by ionizing radiation. L is frequently formed as the 5′-component of tandem lesions generated by radiolysis of DNA whose formation is initiated by radical addition to pyrimidines (25, 26). In *E. coli*, the tandem lesion containing a thymidine glycol flanked on

its 5′-side by L (5′-LTg, Figure 1B), is a much more potent replication block than Tg or L alone and is bypassed only under SOS-induced conditions and is excised by long patch BER (27, 28). Pol β bypasses a single Tg lesion, but all four dNTPs are incorporated opposite the lesion (13). However, the efficiency of incorporation was higher for dATP than for the other nucleotides. Since in this study we showed that Pol β is capable of bypassing a single L lesion on the template, we evaluated the polymerase's ability to bypass the 5′-LTg tandem lesion. Moreover, it has been shown that Pol λ bypasses a single Tg lesion in the template, in contrast to Pol β, in an error-free manner (13). Thus, we asked whether the ability of Pol λ to incorporate dATP opposite Tg was different in the context of a tandem lesion 5′-LTg. To address this question we used a DNA template harboring a two-nucleotide window gap opposite the tandem lesion or the Tg lesion alone (Chart 1, **6** and **7** respectively). When acting on **7**, (Figure 3), Pol β preferentially incorporated dATP opposite the Tg lesion and elongated it, with higher efficiency in the presence of Mn^{2+} than Mg^{2+} (compare Figure 3C lane 2 with Figure 3D lane 2). The nucleotide selectivity of Pol β on **7**, was different from that previously reported (13), confirming the important role of the nature of the nucleobases flanking the Tg lesion, as already noted (29). We found that when part of a tandem lesion, L was a strong block even for Pol β. Furthermore, the oxidized abasic site also affected the bypass efficiency of the preceding thymidine glycol lesion. On this template Pol β incorporated dATP only opposite Tg and was unable to extend the primer past the L lesion (Figure 4A, lanes 6–10). Addition of PCNA did not rescue the bypass activity of pol β toward the second lesion (data not shown). As already noted (13), on substrate **7** Pol λ incorporates only dATP opposite the Tg lesion, with higher efficiency using Mn^{2+} as cofactor than Mg^{2+} (compare Figure 3A, lane 1 with Figure 3B, lane 2). Conversely, it could not incorporate any nucleotide opposite Tg when a L lesion was present downstream from the Tg (**6**) (Figure 4A, lanes 1–5). Three-dimensional structures of Pol λ in complex with 2 nt gapped substrates, have shown that its active site spans template position +1 and +2 with respect to the 3′-OH primer (30). Thus, it is possible that the presence of L at the 5′-side of the Tg lesion prevents proper primer alignment with the incoming nucleotide opposite the Tg lesion.

The ability of L to influence the nucleotide insertion specificity opposite a lesion immediately upstream, as shown above, suggests that L could affect primer binding by polymerases causing distortions in the geometry of the template DNA, thus affecting bypass efficiency irrespective of its base-pairing properties. If true, one might also expect L to affect primer elongation during template-independent primer elongation. Beside Pols λ, β and μ, in human cells the family X polymerases include the enzyme terminal deoxynucleotide transferase (TdT). TdT possesses template-independent polymerase activity, being able to elongate a 3′ end of a DNA strand, independent from the presence of a template strand (18). We thus evaluated the ability of TdT to elongate a recessed 3′-end in the presence of a L at the first position of the 5′-ss overhang (**2**). TdT incorporated all four nucleotides opposite the lesion (Figure 4B, lanes 3–6). Moreover, TdT did not pause after nucleotide incorporation opposite the lesion, extending the newly formed primer with the same efficiency as the undamaged substrate **1** (Figure 4B, compare lane 2 with lanes 7, 8). These data argue against any major distortion of the 3′-end caused by the L lesion and strongly support the notion that L induces enzyme-specific hydrogen bonding with the incoming nucleotide (31). Thus, the oxidized abasic site directly affects nucleotide selectivity and incorporation by template-dependent Pols, without any effect on template-independent enzymes.

Genetic data in yeast suggested that the family B Pol ζ and family Y Rev1 contributed to L bypass *in vivo* (2). Our data suggest that, at least in human cells, also the family X enzyme Pol β has the ability to bypass a L lesion. Yeast cells, contrary to vertebrates, possess only one member of the X family, Pol IV, which thus can be considered the orthologue of both

mammalian Pols λ and β. Given the clear difference between Pol β and λ with respect to L site bypass, we thought of interest to investigate the ability of S. *cerevisiae* Pol IV to overcome such lesion, which is currently unknown. As shown in Figure 4C, Pol IV was able to bypass a single L lesion (**4**), but with virtually no selectivity, incorporating all four nucleotides with similar efficiency. When tested on **6**, bearing the tandem lesion 5′-LTg (Figure 4D), Pol IV incorporated all four nucleotides opposite Tg in the order dATP = dGTP > dTTP > dCTP. Pol IV was also able to elongate from the nucleotide opposite the Tg lesion bypassing the downstream L site, with dGTP being the most efficiently incorporated (Figure 4D, lane 3). Thus, the X family Pol IV in yeast has distinct properties in L site bypass with respect to its human orthologues Pol λ and β and may effectively contribute to mutagenesis consequent to translesion synthesis past this lesion.

These results provide the first direct evidence, to our knowledge, for the ability of the major human DNA repair enzyme Pol β, together with its auxiliary protein PCNA, to bypass a C1′-oxidized abasic site. The presence of a L lesion in the template strand during DNA replication is expected to block replication fork progression. According to the current model for translesion synthesis, a re-priming event downstream from the lesion will allow the fork to resume its advancement, leaving a gap behind to be filled by a specialized Pol. We have shown that Pol β has the ability to incorporate nucleotides opposite L and, together with PCNA, to further elongate the resulting primer end. Thus, bypass of L might be achieved in human cells by the Pol β/PCNA complex. Other than during DNA replication, copying of a template strand containing a L lesion might occur during DNA repair, when gaps are created that need to be filled. For instance, nucleotide excision repair requires the filling of a 30 nt gap, while mismatch repair can require synthesis of long stretches of DNA. In both cases, the replicative enzymes Pols δ and ε are thought to catalyze the resynthesis step. If a L lesion is present on the template, these enzymes might be blocked, causing the accumulation of ss DNA gaps, potentially leading to double-strand DNA breaks. This is particularly important for 2-deoxyribonolactone (L), which is significantly more susceptible to strand scission than an AP site in free or nucleosomal DNA (32–35). Our results might support a role for DNA pol β in rescuing stalled DNA repair complexes as well. The closely related enzyme Pol λ, was, on the other hand, unable to bypass L. Unfortunately, no crystal structures have been solved for any Pol bound to a L containing DNA template, thus the structural basis for this difference remains elusive. Previous studies, however, suggested that the proficiency of *E. coli* Pol V in bypassing L, stems from its ability to stabilize the incoming nucleotide through hydrogen bonding interactions between the carbonyl oxygen (31). Comparison of the active site of Pol β and λ (36), revealed that the Pol β binding pocket for the incoming nucleotide is more tight than the one of Pol λ. Incorporation by Pol β relies on an extensive network of hydrogen bonding interactions with the template base and the incoming nucleotide, essentially made by residues Y271, F272, D276, N279 and R283. On the other hand, Pol λ seems to rely on fewer interactions, mainly due to the R517 residue. Thus, it is possible that the inherent higher flexibility of the Pol λ active site, which favors bypass of other lesions, might be detrimental to L bypass, not allowing the formation of a sufficient network of stabilizing hydrogen bonding interactions. In this context, it is of note that Pol λ bypasses abasic sites mainly through template slippage, generating −1 frameshifts, thanks to its ability to accommodate two template bases in its active site and to stabilize the first one into an extrahelical conformation through interaction with the K544 residue, while Pol β preferentially incorporates dA opposite the abasic site lesion. This behavior is consistent with a higher capability of Pol β in stabilizing an incoming dNTP even in the absence of a templating base. We observed bypass of L lesion by Pol β in the presence of Mg^{2+} only on gapped substrates, while Mn^{2+} was capable of supporting translesion synthesis also on a primer/template structure. It is well known that Mg^{2+} and Mn^{2+} can differentially modulate the catalytic activities of Pols, thus it is entirely possible that, within the cell, their differential usage might be a factor regulating the fidelity and

translesion efficiency of Pols. In our *in vitro* assays we used Mn^{2+} concentrations that are higher than those considered physiologically present in cells. This, however, reflects the high Michelis constant (K_m) of Pol β for this metal ion (16). High K_m values for a cofactor are commonly found in enzymes working in metabolic pathways subjected to tight regulation of the reagents, since working always at subsaturating concentrations enables the enzyme to respond quickly to physiological changes in the concentration of a cofactor. We have shown that Pol β has a dynamic activation range for Mn^{2+} going from 0.1 mM to 5 mM, with the maximal response rate between 0.1 mM and 0.5 mM and near-saturation at 1 mM (16). Thus, Pol β is well suited to be activated by transient increase of Mn^{2+} concentration within the range of physiological values.

Bypass of L by Pol β will be, of course, mutagenic leading in most cases to incorporation of A opposite the lesion. This is consistent with the observation that L is a promutagenic lesion *in vivo* (2, 3). The antitumor drug neocarzinostatin preferentially generates oxidized abasic sites at 2′-deoxycytidine residues (1). The preferential incorporation of dATP opposite L by Pol β is consistent with the frequent GC->AT transitions observed *in vivo* after exposure of cells to neocarzinostatin (37). In addition, since Pol β is overexpressed in many solid tumors (38), our observation may also be relevant to the mechanism of resistance of tumors towards this anticancer drug. Finally, our data show that L in the context of a tandem lesion (such as 5′-LTg) constitutes a strong block even for DNA pol β. It is possible that in such extreme situations another specialized enzyme such as Pol ζ might be needed for the bypass, perhaps in conjunction with Pol β. Furthermore, the biochemical effect of the tandem lesion (5′-LTg) is further evidence for the role that clustered lesions play in the cytotoxicity of ionizing radiation (39, 40).

Methods

Materials and General Methods

Deoxynucleotides were purchased from Gene Spin (Milan, Italy). All the other reagents were of analytical grade and purchased from Fluka or Merck. Oligonucleotides were prepared on an Applied Biosystems Inc. 394 DNA synthesizer. Commercially available DNA synthesis reagents, including the 5*R*,6*S*-thymine glycol phosphoramidite were obtained from Glen Research Inc. Oligonucleotides containing the photolabile 2-deoxyribonolactone precursor were synthesized as previously described (41).

Enzymes and Proteins

Recombinant human PCNA and Pol λ were expressed in *E. coli* and purified as previously described (15). Recombinant human Pol β and TdT were from Trevigen Inc. (Gaithersburg, MD 20877 USA). *S. cerevisiae* Pol IV was a gift of Dr. Stephane Marcand, CEA/Fontenay (France).

DNA substrates

The 15-mer oligonucleotide primer was radioactively labeled at its 5′-end by T4 polynucleotide kinase and [γ-^{33}P] ATP, according to manufacturer's protocols. All oligonucleotides were mixed in equimolar amounts in the presence of 25 mM TrisHCl pH 8 and 50 mM KCl, heated at 75°C for 10 min and then slowly cooled down at room temperature, to generate substrates **1** – **7** (Chart 1). After oligonucleotide annealing, L was activated by UV irradiation (365 nM) for two hours in ice. L activation was checked by alkali-induced DNA cleavage by addition of 0.1 M NaOH at 37°C for 30 min followed by neutralization with formic acid. Oligonucleotide cleavage was checked by polyacrylamide gel electrophoresis.

In vitro translesion synthesis assays

For denaturing gel analysis of the DNA products, the reaction mixtures (10 μl) contained: 50 mM Tris-HCl pH 7.5, 1mM DTT, 0.20 mg/ml BSA, 2% glycerol, 0.1 pmols of 5′-^{33}P labeled DNA substrates. Enzymes, Mg^{2+}, Mn^{2+}, dNTPs and purified PCNA were as indicated in the Figure legends. Reaction mixtures were incubated for 10 min at 37°C and then stopped by addition of standard denaturing gel loading buffer (95% formamide, 10 mM EDTA, xylene cyanol and bromophenol blue), heated at 95°C for 5 min and loaded on a 7 M urea 12% polyacrylamide gel. The reaction products were analyzed by using Molecular Dynamics Phosphoimager (Typhoo Trio GE Healthcare) and quantified by Image Quant and GraphPad Prism programs.

Steady-state kinetic analysis

The initial velocity of the reaction was calculated (Image Quant and GraphPad Prism 3.0) from the values of integrated gel band intensities:

$$I^*_T/I_{T-1},$$

where T is the target site, the template position of interest; I^*_T is the sum of the integrated intensities at positions T, T +1, …, T + n.

All of the intensity values were normalized to the total intensity of the corresponding lane to correct for differences in gel loading. The apparent K_m and V_{max} values were calculated by plotting the initial velocities in dependence of the nucleotide [dNTP] or primer [3′-OH] substrate concentrations and fitting the data according to Michaelis- Menten equation:

$$I^*_T/I_{T-1}=V_{max}/(1+K_m/[S]),$$

where [S] was the variable substrate. Substrate incorporation efficiencies were defined as the V_{max}/K_m ratio.

Acknowledgments

This work has been partially supported by the Italian Association for Cancer Research AIRC (IG grant 12084) and the Superpig Program, project co-financed by Lombardy Region through the “Fund for promoting institutional agreements”, to GM and the National Institute of General Medical Sciences (GM-063028) to MMG.

References

1. Kappen LS, Goldberg IH. Identification of 2-deoxyribonolactone at the site of neocarzinostatin-induced cytosine release in the sequence d(AGC). Biochemistry. 1989; 28:1027–1032. [PubMed: 2523732]
2. Kroeger KM, Jiang YL, Kow YW, Goodman MF, Greenberg MM. Mutagenic effects of 2-deoxyribonolactone in Escherichia coli. An abasic lesion that disobeys the A-rule. Biochemistry. 2004; 43:6723–6733. [PubMed: 15157106]
3. Kow YW, Bao G, Minesinger B, Jinks-Robertson S, Siede W, Jiang YL, Greenberg MM. Mutagenic effects of abasic and oxidized abasic lesions in Saccharomyces cerevisiae. Nucleic Acids Res. 2005; 33:6196–6202. [PubMed: 16257982]
4. San Pedro JM, Beerman TA, Greenberg MM. DNA damage by C1027 involves hydrogen atom abstraction and addition to nucleobases. Bioorg Med Chem. 2012; 20:4744–4750. [PubMed: 22748380]
5. Hashimoto M, Greenberg MM, Kow YW, Hwang JT, Cunningham RP. The 2-deoxyribonolactone lesion produced in DNA by neocarzinostatin and other damaging agents forms cross-links with the

base-excision repair enzyme endonuclease III. J Am Chem Soc. 2001; 123:3161–3162. [PubMed: 11457038]

6. DeMott MS, Beyret E, Wong D, Bales BC, Hwang JT, Greenberg MM, Demple B. Covalent trapping of human DNA polymerase beta by the oxidative DNA lesion 2-deoxyribonolactone. J Biol Chem. 2002; 277:7637–7640. [PubMed: 11805079]
7. Kroeger KM, Hashimoto M, Kow YW, Greenberg MM. Cross-linking of 2- deoxyribonolactone and its beta-elimination product by base excision repair enzymes. Biochemistry. 2003; 42:2449–2455. [PubMed: 12600212]
8. Ide H, Kotera M. Human DNA glycosylases involved in the repair of oxidatively damaged DNA. Biol Pharm Bull. 2004; 27:480–485. [PubMed: 15056851]
9. Sung JS, DeMott MS, Demple B. Long-patch base excision DNA repair of 2- deoxyribonolactone prevents the formation of DNA-protein cross-links with DNA polymerase beta. J Biol Chem. 2005; 280:39095–39103. [PubMed: 16188889]
10. Sung JS, Demple B. Roles of base excision repair subpathways in correcting oxidized abasic sites in DNA. Febs J. 2006; 273:1620–1629. [PubMed: 16623699]
11. Liu P, Qian L, Sung JS, de Souza-Pinto NC, Zheng L, Bogenhagen DF, Bohr VA, Wilson DM 3rd, Shen B, Demple B. Removal of oxidative DNA damage via FEN1-dependent long-patch base excision repair in human cell mitochondria. Mol Cell Biol. 2008; 28:4975–4987. [PubMed: 18541666]
12. Blanca G, Villani G, Shevelev I, Ramadan K, Spadari S, Hubscher U, Maga G. Human DNA polymerases lambda and beta show different efficiencies of translesion DNA synthesis past abasic sites and alternative mechanisms for frameshift generation. Biochemistry. 2004; 43:11605–11615. [PubMed: 15350147]
13. Belousova EA, Maga G, Fan Y, Kubareva EA, Romanova EA, Lebedeva NA, Oretskaya TS, Lavrik OI. DNA polymerases beta and lambda bypass thymine glycol in gapped DNA structures. Biochemistry. 2010; 49:4695–4704. [PubMed: 20423048]
14. Crespan E, Hubscher U, Maga G. Error-free bypass of 2-hydroxyadenine by human DNA polymerase lambda with Proliferating Cell Nuclear Antigen and Replication Protein A in different sequence contexts. Nucleic Acids Res. 2007; 35:5173–5181. [PubMed: 17666409]
15. Maga G, Villani G, Crespan E, Wimmer U, Ferrari E, Bertocci B, Hubscher U. 8-oxo-guanine bypass by human DNA polymerases in the presence of auxiliary proteins. Nature. 2007; 447:606–608. [PubMed: 17507928]
16. Blanca G, Shevelev I, Ramadan K, Villani G, Spadari S, Hubscher U, Maga G. Human DNA polymerase lambda diverged in evolution from DNA polymerase beta toward specific Mn(++) dependence: a kinetic and thermodynamic study. Biochemistry. 2003; 42:7467–7476. [PubMed: 12809503]
17. Cisneros GA, Perera L, Garcia-Diaz M, Bebenek K, Kunkel TA, Pedersen LG. Catalytic mechanism of human DNA polymerase lambda with Mg2+ and Mn2+ from ab initio quantum mechanical/molecular mechanical studies. DNA Repair (Amst). 2008; 7:1824–1834. [PubMed: 18692600]
18. Hubscher U, Maga G, Spadari S. Eukaryotic DNA polymerases. Annu Rev Biochem. 2002; 71:133–163. [PubMed: 12045093]
19. Duym WW, Fiala KA, Bhatt N, Suo Z. Kinetic effect of a downstream strand and its 5′-terminal moieties on single nucleotide gap-filling synthesis catalyzed by human DNA polymerase lambda. J Biol Chem. 2006; 281:35649–35655. [PubMed: 17005572]
20. Maga G, Crespan E, Wimmer U, van Loon B, Amoroso A, Mondello C, Belgiovine C, Ferrari E, Locatelli G, Villani G, Hubscher U. Replication protein A and proliferating cell nuclear antigen coordinate DNA polymerase selection in 8-oxo-guanine repair. Proc Natl Acad Sci U S A. 2008; 105:20689–20694. [PubMed: 19104052]
21. Fiala KA, Duym WW, Zhang J, Suo Z. Up-regulation of the fidelity of human DNA polymerase lambda by its non-enzymatic proline-rich domain. J Biol Chem. 2006; 281:19038–19044. [PubMed: 16675458]
22. Maga G, Villani G, Ramadan K, Shevelev I, Tanguy Le Gac N, Blanco L, Blanca G, Spadari S, Hubscher U. Human DNA polymerase lambda functionally and physically interacts with

proliferating cell nuclear antigen in normal and translesion DNA synthesis. J Biol Chem. 2002; 277:48434–48440. [PubMed: 12368291]

23. Kedar PS, Kim SJ, Robertson A, Hou E, Prasad R, Horton JK, Wilson SH. Direct interaction between mammalian DNA polymerase beta and proliferating cell nuclear antigen. J Biol Chem. 2002; 277:31115–31123. [PubMed: 12063248]
24. Maga G, van Loon B, Crespan E, Villani G, Hubscher U. The block of DNA polymerase delta strand displacement activity by an abasic site can be rescued by the concerted action of DNA polymerase beta and Flap endonuclease 1. J Biol Chem. 2009; 284:14267–14275. [PubMed: 19329428]
25. Carter KN, Greenberg MM. Tandem lesions are the major products resulting from a pyrimidine nucleobase radical. J Am Chem Soc. 2003; 125:13376–13378. [PubMed: 14583031]
26. Hong IS, Carter KN, Sato K, Greenberg MM. Characterization and mechanism of formation of tandem lesions in DNA by a nucleobase peroxyl radical. J Am Chem Soc. 2007; 129:4089–4098. [PubMed: 17335214]
27. Huang H, Imoto S, Greenberg MM. The mutagenicity of thymidine glycol in Escherichia coli is increased when it is part of a tandem lesion. Biochemistry. 2009; 48:7833–41. [PubMed: 19618962]
28. Imoto S, Bransfield LA, Croteau DL, Van Houten B, Greenberg MM. DNA Tandem Lesion Repair by Strand Displacement Synthesis and Nucleotide Excision Repair. Biochemistry. 2008; 47:4306–4316. [PubMed: 18341293]
29. Aller P, Duclos S, Wallace SS, Doublié SA. Crystallographic study of the role of sequence context in thymine glycol bypass by a replicative DNA polymerase serendipitously sheds light on the exonuclease complex. J Mol Biol. 2011; 412:22–34. [PubMed: 21781974]
30. Garcia-Diaz M, Bebenek K, Larrea AA, Havener JM, Perera L, Krahn JM, Pedersen LC, Ramsden DA, Kunkel TA. Template strand scrunching during DNA gap repair synthesis by human polymerase lambda. Nat Struct Mol Biol. 2009; 16:967–972. [PubMed: 19701199]
31. Huang H, Greenberg MM. Hydrogen bonding contributes to the selectivity of nucleotide incorporation opposite an oxidized abasic lesion. J Am Chem Soc. 2008; 130:6080–6081. [PubMed: 18412345]
32. Zheng Y, Sheppard TL. Half-life and DNA strand scission products of 2-deoxyribonolactone oxidative DNA damage lesions. Chem Res Toxicol. 2004; 17:197–207. [PubMed: 14967007]
33. Roupioz Y, Lhomme J, Kotera M. Chemistry of the 2-deoxyribonolactone lesion in oligonucleotides: cleavage kinetics and products analysis. J Am Chem Soc. 2002; 124:9129–9135. [PubMed: 12149017]
34. Sczepanski JT, Wong RS, McKnight JN, Bowman GD, Greenberg MM. Rapid DNA-protein cross-linking and strand scission by an abasic site in a nucleosome core particle. Proc Natl Acad Sci U S A. 2010; 107:22475–22480. [PubMed: 21149689]
35. Zhou C, Greenberg MM. Histone-catalyzed cleavage of nucleosomal DNA containing 2-deoxyribonolactone. J Am Chem Soc. 2012; 134:8090–8093. [PubMed: 22551239]
36. Moon AF, Garcia-Diaz M, Batra VK, Beard WA, Bebenek K, Kunkel TA, Wilson SH, Pedersen LC. The X family portrait: structural insights into biological functions of X family polymerases. DNA Repair (Amst). 2007; 6:1709–1725. [PubMed: 17631059]
37. Povirk LF, Goldberg IH. Base substitution mutations induced in the cI gene of lambda phage by neocarzinostatin chromophore: correlation with depyrimidination hotspots at the sequence AGC. Nucleic Acids Res. 1986; 14:1417–1426. [PubMed: 2937016]
38. Albertella MR, Lau A, O'Connor MJ. The overexpression of specialized DNA polymerases in cancer. DNA Repair (Amst). 2005; 4:583–593. [PubMed: 15811630]
39. Sage E, Harrison L. Clustered DNA Lesion Repair in Eukaryotes: Relevance to Mutagenesis and Cell Survival. Mutat Res. 2011; 711:123–133. [PubMed: 21185841]
40. O'Neill P, Wardman P. Radiation Chemistry Comes before Radiation Biology. Int J Radiat Biol. 2009; 85:9–25. [PubMed: 19205982]
41. Kotera M, Roupioz Y, Defrancq E, Bourdat AG, Garcia J, Coulombeau C, Lhomme J. The 7-nitroindole nucleoside as a photochemical precursor of 2′-deoxyribonolactone: access to DNA

fragments containing this oxidative abasic lesion. Chemistry. 2000; 6:4163–4169. [PubMed: 11128280]

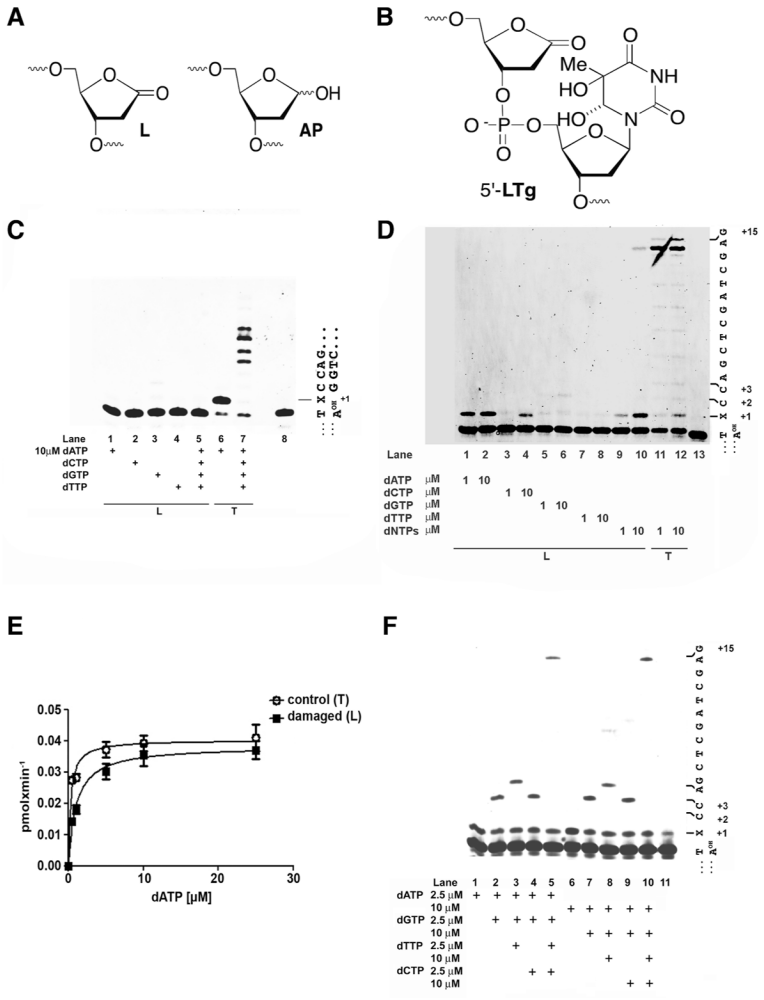

Figure 1.

DNA polymerase β, but not λ, can bypass a L lesion. (A). Structure of the oxidized (L) and normal (AP) abasic site. (B). Structure of the tandem lesion 5′-LTg. (C.) Nucleotide incorporation by Pol λ was measured in the presence of different nucleotides concentration, 0.1 pmol of substrate **3** (lanes 6, 7) or substrate **4** (lanes 1–5) and 2.5 mM Mn^{2+}. Lane 8: 5′-^{32}P-labeled DNA primer (15 nt). (D.) Nucleotide incorporation by Pol β (100 nM) was measured in the presence of different nucleotides concentration, 0.1 pmol of substrate **1** (lanes 11–12) or substrate **2** (lanes 1–10) and 2.5 mM Mn^{2+}. Lane 13: 5′-^{32}P-labeled DNA primer (15 nt). (E). Variation of the reaction velocity of Pol β as a function of dATP concentrations. Reactions were performed in the presence of 100 nM Pol β, 2.5 mM Mn^{2+} and 0.1 pmol of substrate **1** (empty circles) or substrate **2** (filled squares). Values are the means of three independent experiments. Error bars represent ± S.D. (F). DNA primer elongation by Pol β (100 nM) was measured, using different amounts and combination of nucleotides, 0.1 pmol of substrate 2 and 2.5 mM Mn^{2+}. Lane 11: 5′-^{32}P-labeled DNA primer (15 nt). The sequence of the DNA template is indicated on the right side of the panel.

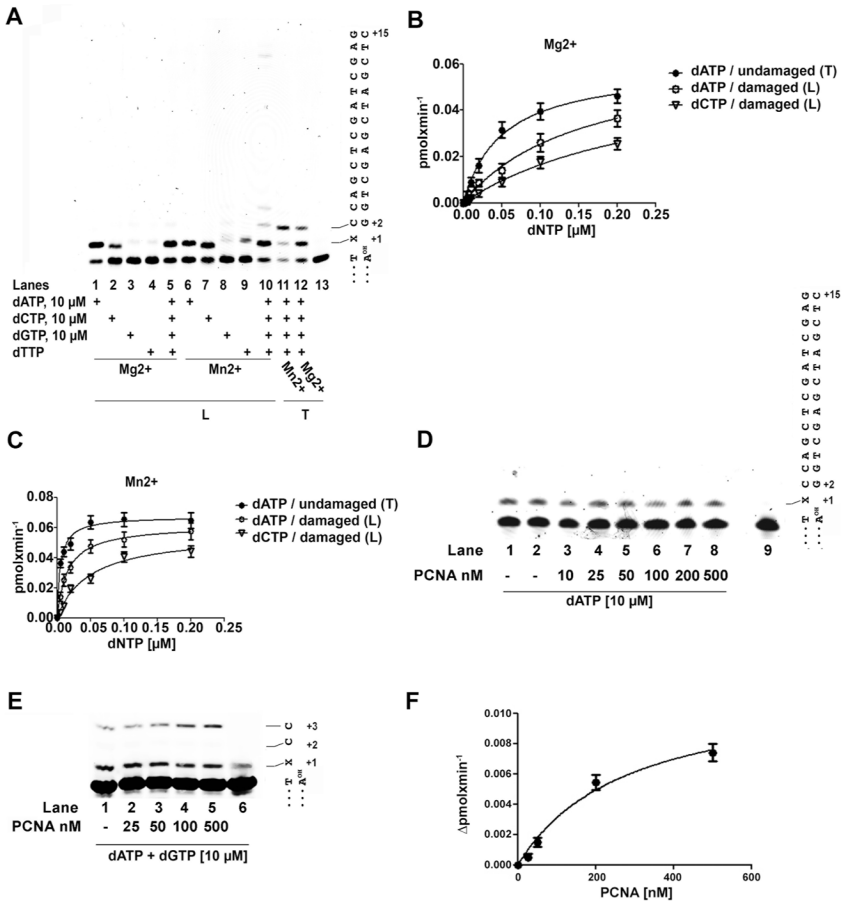

Figure 2.

Nucleotide insertion specificity and stimulation by PCNA of Pol β bypass of a L lesion. (A.) Nucleotide incorporation by Pol β (100 nM) was measured in the presence of different nucleotides concentration, 0.1 pmol of substrate **3** (lanes 11–12) or substrate **4** (lanes 1–10) and 2.5 mM Mg^{2+} (lanes 1–5, 12) or 2.5 mM Mn^{2+} (lanes 6–10, 11). Lane 13: 5′-^{32}P-labeled DNA primer (15 nt). (B.) Variation of the reaction velocity of Pol β as a function of nucleotide concentration. Reactions were performed as described in Materials and Methods in the presence of 2.5 mM Mg^{2+}, 0.1 pmol of substrate **3** and increasing amounts of dATP (filled circles), or substrate **4** and increasing amount of dATP (empty circles) or dCTP (empty triangles). Values are the means of three independent experiments. Error bars represent ± S.D. (C.) As in panel B, but in the presence of 2.5 mM Mn^{2+}. (D.) Nucleotide incorporation by Pol β (100 nM) was measured, in the presence of 0.1 pmol of substrate **4**, 10 μM dATP, 2.5 mM Mn^{2+} and increasing amounts of PCNA. The sequence of the DNA template is indicated on the right side of the panel. Lane 9: 5′-^{32}P-labeled DNA primer (15 nt). (E.) As in panel D, but in the presence of substrate **2** and 10 μM dATP and dGTP. (F). Increase (Δ) in the reaction velocity of Pol β as a function of PCNA concentration. Values are the means of three independent experiments. Error bars represent ± S.D. Data were fitted to the equation $\Delta obs = \Delta max/(1+K_d/[PCNA])$.

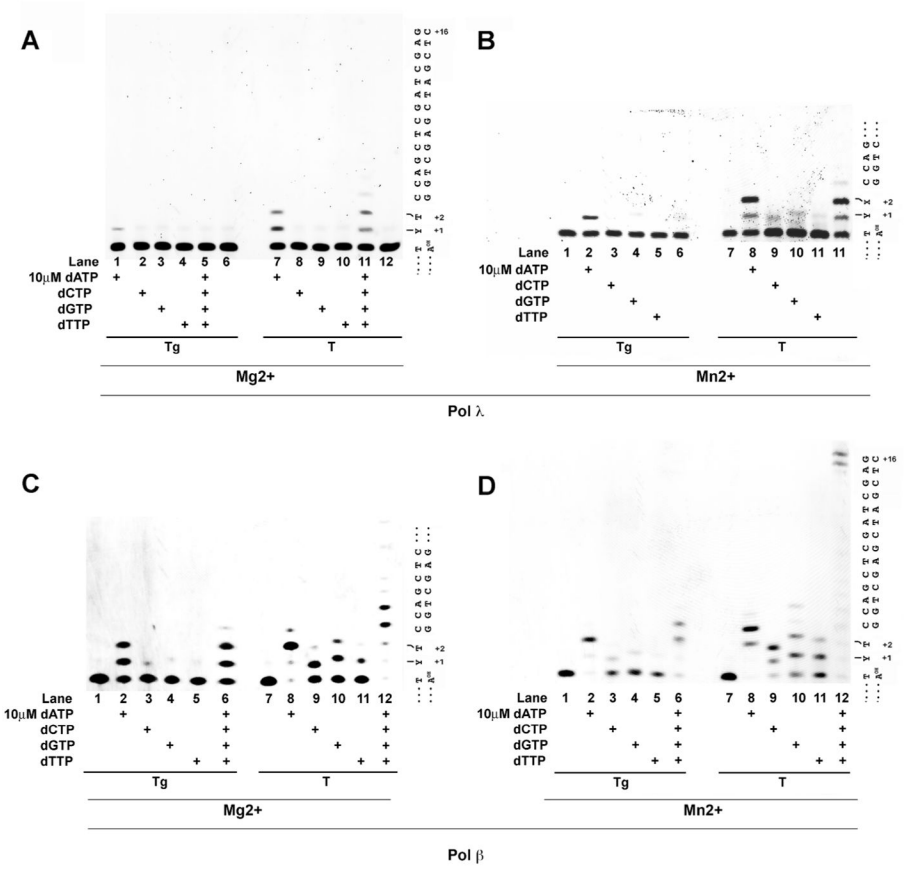

Figure 3.

(A) Nucleotide incorporation by 100 nM of Pol λ (lanes 1–5, 7–11) was measured in the presence of different nucleotides, 0.1 pmol of substrate 7 (lanes 1–5) or substrate 5 (lanes 7–11) and 2.5 mM Mg^{2+}. Lane 6–12: 5′-^{32}P-labeled DNA primer (14 nt). (B) Nucleotide incorporation by 100 nM of Pol λ (lanes 2–6, 8–12) was measured in the presence of different nucleotides, 0.1 pmol of substrate 7 (lanes 2–6) or substrate 5 (lanes 8–12) and 2.5 mM Mn^{2+}. Lane 1–7: 5′-^{32}P-labeled DNA primer (14 nt). (C) Nucleotide incorporation by 100 nM of Pol β (lanes 2–6, 8–12) was measured in the presence of different nucleotides, 0.1 pmol of substrate 7 (lanes 2–6) or substrate 5 (lanes 8–12) and 2.5 mM Mg^{2+}. Lane 1–7: 5′-^{32}P-labeled DNA primer (14 nt). (D) Nucleotide incorporation by 100 nM of Pol β (lanes 2–6, 8–12) was measured in the presence of different nucleotides, 0.1 pmol of substrate 7 (lanes 2–6) or substrate 5 (lanes 8–12) and 2.5 mM Mn^{2+}. Lane 1–7: 5′-^{32}P-labeled DNA primer (14 nt).

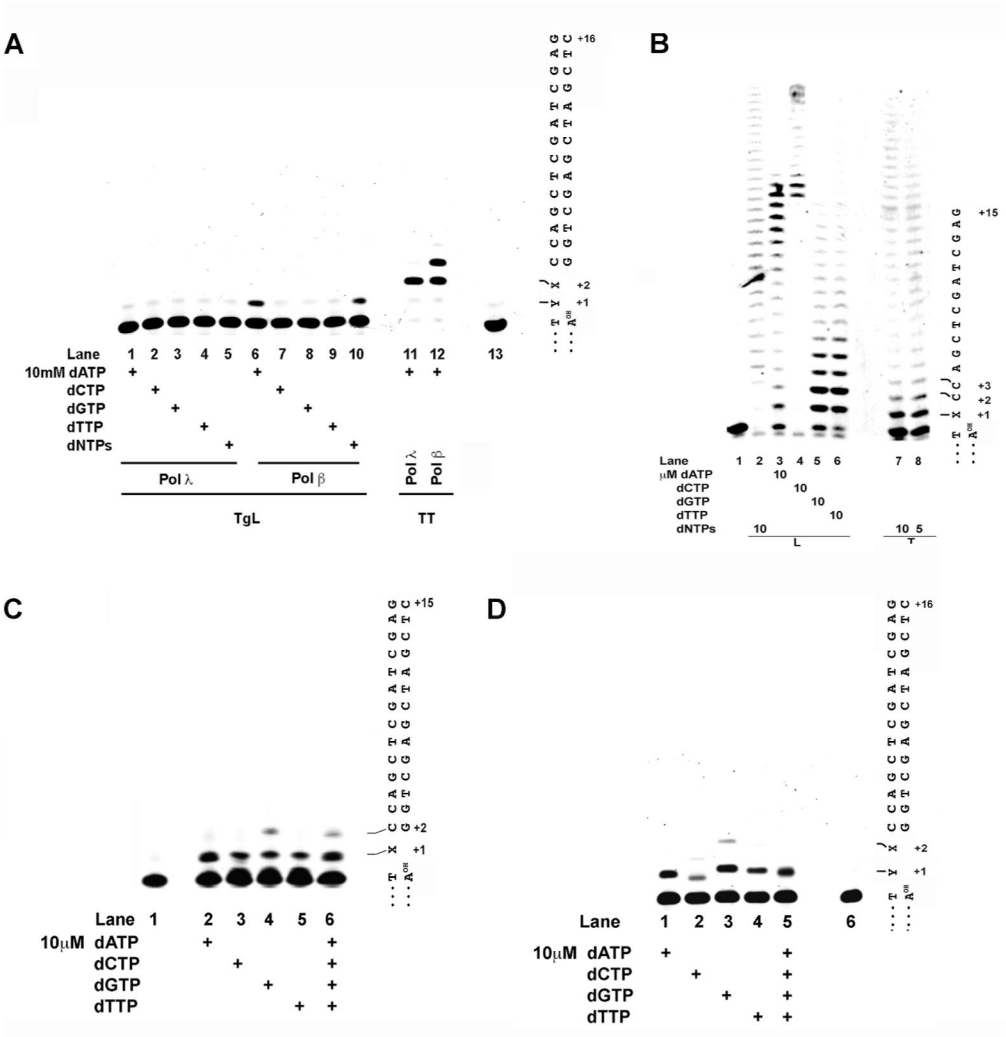

Figure 4.

A tandem 5′-LTg lesion constitutes a strong block for human Pols β and λ, but not for *S.cerevisiae* Pol IV. (A) Nucleotide incorporation by 100 nM of Pol λ (lanes 1–5, 11) or Pol β (lanes 6–10, 12), was measured in the presence of different nucleotides, 0.1 pmol of substrate **5** (lanes 11–12) or substrate **6** (lanes 1–10) and 2.5 mM Mn^{2+}. Lane 13: 5′-^{32}P-labeled DNA primer (15 nt). (B) Nucleotide incorporation by 100 nM TdT was measured as described in Materials and Methods, in the presence of different nucleotides, 0.1 pmol of substrate **1** (lanes 7–8) or substrate **2** (lanes 2–6) and 2.5 mM Mn^{2+}. Lane 1: 5′-^{32}P-labeled DNA primer (15 nt). The sequence of the DNA template is indicated on the right side of the panel. (C) Nucleotide incorporation by 100 nM Pol IV was measured in the presence of different nucleotides, 0.1 pmol of substrate **4** and 2.5 mM Mn^{2+}. Lane 1: 5′-^{32}Plabeled DNA primer (15 nt). (D). Nucleotide incorporation by Pol IV was measured in the presence of different nucleotides, 0.1 pmol of substrate **6** and 2.5 mM Mn^{2+}. Lane 6: 5′-^{32}P-labeled DNA primer (15 nt).

AAT CCT GGA CGT CGA-5'
GAG CTA GCT CGA CC**X** TTA GGA CCT GCA GCT-3'

1 **X** = T
2 **X** = L

CTC GAT CGA GCT GG AAT CCT GGA CGT CGA-5'
GAG CTA GCT CGA CC **X** TTA GGA CCT GCA GCT-3'

3 **X** = T
4 **X** = L

CTC GAT CGA GCT GG AT CCT GGA CGT CGA-5'
GAG CTA GCT CGA CC **X** **Y**TA GGA CCT GCA GCT-3'

5 **X** = **Y** = T
6 **X** = L, **Y** = Tg
7 **X** = T, **Y** = Tg

Chart 1.

Table 1

Kinetic parameters for single nucleotide incorporation on primer/template or single nucleotide gapped DNA substrates by DNA polymerase β.

	Mg^{2+}			Mn^{2+}		
DNA substrate/incoming nucleotide	**Vmax[a] (pmol•min^{-1})**	**Km (μM)**	**Vmax/Km**	**Vmax (pmol•min^{-1})**	**Km (μM)**	**Vmax/Km**
1/dATP[b]	n.d.[b]	n.d.	n.d.	0.041 ± 0.002	0.26 ± 0.02	0.15
2/dATP	n.d.	n.d.	n.d.	0.038 ± 0.003	1.01 ± 0.01	0.04
3/dATP	0.06 ± 0.01	0.05 ± 0.01	1.2	0.067 ± 0.07	0.015 ± 0.002	4.4
4/dATP	0.06 ± 0.006	0.35 ± 0.03	0.17	0.06 ± 0.01	0.29 ± 0.02	0.2
4/dCTP	0.049 ± 0.005	0.88 ± 0.07	0.055	0.053 ± 0.005	0.65 ± 0.05	0.08

[a]Kinetic parameters Vmax and Km were determined as described in Materials and Methods. Values are the means of three independent experiments ± S.D. b. n.d., not determined.

[b]DNA substrates are numbered as in Chart 1.